

Disorder-induced localisation in the Mott-Hubbard model

R. Kristers Knipšis,^{1,2} F. Queisser,^{1,2} J. Jayabalan,³ G. Reecht,³ M. Gruber,³ U. Bovensiepen,³ and R. Schützhold^{1,2}

¹*Helmholtz-Zentrum Dresden-Rossendorf, Bautzner Landstraße 400, 01328 Dresden, Germany*

²*Institut für Theoretische Physik, Technische Universität Dresden, 01062 Dresden, Germany*

³*Fakultät für Physik und Center for Nanointegration (CENIDE), Universität Duisburg-Essen, Lotharstr. 1, 47057 Duisburg, Germany*

(Dated: March 12, 2026)

For the Fermi-Hubbard model in the Mott insulator phase, we employ the hierarchy of correlations to study how doublon and holon quasi-particle excitations are affected by adding disorder to the system. We study two types of disorder: charge disorder, in the form of on-site potential randomness; and spin disorder, in the form of a fixed, randomly generated background spin arrangement. By analysing the quasi-particle eigen-spectra and quantifying the degree to which the corresponding eigen-states localise, we find both an energetic and spatial separation between localised and delocalised states in the charge disorder. In contrast, the spin disorder results in localised states throughout the quasi-particle bands. Finally, we repeat our calculations using strong-coupling perturbation theory, and compare the results obtained from both methods.

I. INTRODUCTION

Going from textbooks to real life, one quickly finds the perfectly ordered systems of the former affected to varying degrees of imperfections and disorder in the latter. This has historically been an unwanted effect to be eliminated or worked around. In recent decades, however, as the interest in suppressing thermalisation in quantum systems has grown, considerable attention has been paid to disordered systems.

In Anderson's seminal paper [1], it was argued that an on-site disorder can localise non-interacting particles in a lattice, eliminating long-range transport in the system at zero temperature. Subsequently, the same conclusion was extended to weakly interacting systems [2]. Since then, localisation has been observed in various photonic [3–5], acoustic [6, 7], and matter systems with suppressed inter-particle interactions [8, 9].

On the other hand, it was long unclear whether localisation would survive in a strongly interacting system at nonzero temperatures. An answer to the affirmative has been suggested in the form of many-body localisation (MBL), where the existence of quasi-local integrals of motion point towards ergodicity breaking even at finite temperatures [10–13]. This remarkable theory quickly gained experimental support [14]. On the other hand, coupling to phonon baths is known to destroy MBL, and it is also disputed whether the MBL phase is stable in more than one dimension.

Motivated by these questions, our starting point is the Fermi-Hubbard model [15] in a 2D lattice

$$\hat{H} = -\frac{1}{Z} \sum_{\mu,\nu,s} T_{\mu\nu} \hat{c}_{\mu,s}^\dagger \hat{c}_{\nu,s} + U \sum_{\mu} \hat{n}_{\mu,\uparrow} \hat{n}_{\mu,\downarrow}, \quad (1)$$

where μ, ν are site indices, $T_{\mu\nu} = T$ for nearest neighbour sites and zero otherwise, Z is the coordination number of the lattice, $\hat{c}_{\mu,s}^\dagger$ ($\hat{c}_{\mu,s}$) is the creation (annihilation) operator for an electron of spin s at site μ , and U is the on-site interaction energy.

II. SETUP

We consider two-dimensional lattices with different coordination numbers, namely, the hexagonal ($Z = 6$), square ($Z = 4$), and honeycomb ($Z = 3$) lattices. Throughout this paper, we enforce periodic boundary conditions, and only consider lattices with equal sizes in both dimensions, $N = N_x = N_y$, and, unless stated otherwise, we take $N = 25$. Note that $\hbar = 1$ throughout this paper.

We consider the limit of weak hopping strength $T \ll U$, such that also $T \gg T^2/U$. We restrict our considerations to timescales $\sim 1/T$, and in particular such that we do not reach the spin dynamics timescale $\sim U/T^2$. This ensures that the spin backgrounds considered in this paper can be well approximated to be static.

In this paper, we consider two types of disorder, namely, charge disorder and spin disorder. The former is defined by a spin-independent on-site potential,

$$\hat{H}_c = \sum_{\mu} V_{\mu} (\hat{n}_{\mu,\uparrow} + \hat{n}_{\mu,\downarrow}), \quad (2)$$

where V_{μ} is assigned with probability r to each lattice site to be either 0 or V . This is in contrast to typical Anderson localisation where V_{μ} is sampled from a continuous distribution.

Meanwhile, spin disorder is defined by an on-site potential that introduces a spin-splitting,

$$\hat{H}_s = \sum_{\mu} v_{\mu} (\hat{n}_{\mu,\uparrow} - \hat{n}_{\mu,\downarrow}), \quad (3)$$

where $v_{\mu} \in \{-v, v\}$ is again randomly chosen at each site, thereby energetically favouring a particular spin-orientation. We choose $T \gg v \gg T^2/U$, such that spin dynamics are frozen in the timescales considered in this paper. In practice, to make calculations tractable, the spin-splitting is imposed implicitly by only considering states in the lowest energy subspace. Consequently, it should be kept in mind that the corresponding results only hold on sufficiently short timescales.

III. HIERARCHY OF CORRELATIONS

A. Factorised equations of motion

The hierarchy of correlations is an expansion in orders of $1/Z$ where $Z \gg 1$ is the coordination number of the lattice [16]. In this paper we are interested in one-point density matrices and two-point correlators, in other words, the objects of interest are the reduced density matrices $\hat{\rho}_\mu$ and $\hat{\rho}_{\mu\nu}$. In fact, a hierarchy in orders of $1/Z$ requires considering only the correlated parts of the density matrices. For instance, the two-point object of interest is $\hat{\rho}_{\mu\nu}^{corr} = \hat{\rho}_{\mu\nu} - \hat{\rho}_\mu \hat{\rho}_\nu$, the three-point reduced density matrix of interest would be $\hat{\rho}_{\mu\nu\lambda}^{corr} = \hat{\rho}_{\mu\nu\lambda} - \hat{\rho}_\mu \hat{\rho}_\nu \hat{\rho}_\lambda - \hat{\rho}_{\mu\nu}^{corr} \hat{\rho}_\lambda - \hat{\rho}_{\mu\lambda}^{corr} \hat{\rho}_\nu - \hat{\rho}_{\nu\lambda}^{corr} \hat{\rho}_\mu$, and so on.

Then, the time evolution of the relevant density matrices follows the hierarchy [16]

$$i\partial_t \hat{\rho}_\mu = f_1(\hat{\rho}_\mu, \hat{\rho}_{\mu\nu}^{corr}) \sim \mathcal{O}(1), \quad (4)$$

$$i\partial_t \hat{\rho}_{\mu\nu}^{corr} = f_2(\hat{\rho}_\mu, \hat{\rho}_{\mu\nu}^{corr}, \hat{\rho}_{\mu\nu\lambda}^{corr}) \sim \mathcal{O}(1/Z). \quad (5)$$

In fact, as long as the density matrices also meet corresponding initial conditions $\hat{\rho}_\mu \sim \mathcal{O}(1)$, $\hat{\rho}_{\mu\nu}^{corr} \sim \mathcal{O}(1/Z)$ and so on, this hierarchy is also conserved at subsequent times limited only by the growth of unstable modes (if present) [16]. This observation allows us to truncate to a particular order in $1/Z$. In this paper, we truncate to first order $1/Z$, meaning that the contributions of all density matrices beyond two-point can be neglected.

At this point, we can specify the correlators of interest. When considering quasi-particles on a half-filled background, the relevant operators are the dressed fermionic operators

$$\hat{C}_{\mu,s}^I = \hat{N}_{\mu,\bar{s}}^I \hat{c}_{\mu,s} = \begin{cases} \hat{n}_{\mu,\bar{s}} \hat{c}_{\mu,s} & I = 1, \\ (1 - \hat{n}_{\mu,\bar{s}}) \hat{c}_{\mu,s} & I = 0, \end{cases} \quad (6)$$

which act as precursors for holon ($I = 0$) and doublon ($I = 1$) quasiparticles.

We now consider the two-point correlators $\langle \hat{C}_{\mu,s}^{I\dagger} \hat{C}_{\nu,s}^J \rangle^{corr}$. In fact, to first order $1/Z$, we can equivalently employ the factorisation ansatz [17] to write

$$\langle \hat{C}_{\mu,s}^{I\dagger} \hat{C}_{\nu,s}^J \rangle^{corr} = (p_{\mu,s}^I)^* p_{\nu,s}^J \quad (7)$$

such that to get the time dependence of $\langle \hat{C}_{\mu,s}^{I\dagger} \hat{C}_{\nu,s}^J \rangle^{corr}$ we need only to solve the much simpler set of equations

$$i\partial_t p_{\mu,s}^I = U^I p_{\mu,s}^I - \frac{1}{Z} \sum_{\nu,X} T_{\nu\mu} \langle \hat{N}_{\mu,\bar{s}}^I \rangle^0 p_{\nu,s}^X, \quad (8)$$

where to our order of approximation, $\langle \hat{N}_{\mu,\bar{s}}^I \rangle \approx \langle \hat{N}_{\mu,\bar{s}}^I \rangle^0$ is sufficiently approximated to order $\mathcal{O}(1)$. A similar equation could be found using other approximation schemes, e.g. [18].

Solving the above, we obtain holon (dominated by the $p_{\mu,s}^0$ contributions) and doublon (dominated by the $p_{\mu,s}^1$ contributions, with energies centred around U) eigenstates and eigen-energies. Note that the holon energies are actually minus the corresponding eigen-energies.

In order to explicitly study the effects of different lattice geometries, we keep T/Z constant between lattices.

B. Charge disorder

We consider a system at half-filling in the large- U limit. This imposes that every lattice site has one fermion, but the spin direction is not fixed. Thus, as a starting point, we assume the same statistic mixture of the two spin states at each lattice site

$$\hat{\rho}_\mu^0 = \frac{1}{2} \left(|\uparrow\rangle_\mu \langle \uparrow| + |\downarrow\rangle_\mu \langle \downarrow| \right). \quad (9)$$

This immediately gives that $\langle \hat{N}_{\mu,\bar{s}}^I \rangle^0 = 1/2$ in equation (8). Adding the charge disorder of equation (2), quasi-particles are now described by

$$i\partial_t p_{\mu,s}^I = (U^I + V_\mu) p_{\mu,s}^I - \frac{1}{2Z} \sum_{\nu,X} T_{\nu\mu} p_{\nu,s}^X, \quad (10)$$

which we solve numerically.

In the following, we fix $U = 0.35$ eV and $T/Z = 0.05$ eV. Eigen-spectra for $V \in \{0.00, -0.10, -0.20\}$ eV for identical charge distributions are shown in Figure 1. Note that we observe the splitting of holon and doublon bands into sub-bands, separated in energy by the on-site potential strength V .

We can take a step further and also characterise the eigen-states by how localised they are. A simple quantifier for this is the inverse participation ratio (IPR), defined in our case by the functional [19, 20]

$$\text{IPR}\{p(E_n)\} = \sum_{\mu,I} |p_\mu^I(E_n)|^4. \quad (11)$$

The inverse of the IPR, the participation ratio, describes the number of sites over which a state extends [19]. Thus, for our normalised ‘eigen-states’ this is bounded by $1 < \text{IPR}^{-1} < 2N^2$. We can use this to colour the spectrum by classifying states into localised and delocalised states depending on their participation ratio i.e. ‘number of sites they cover on the lattice’. From e.g. Figure 2, we see that the emerging sub-bands are predominantly composed of localised states, while the remains of the original bands are predominantly delocalised. Intuitively, in the limit where only a small fraction of sites are affected by the charge disorder, only a small number of the free quasi-particle states will be pinned down by the disorder, the rest remaining as free, plane-wave-like states.

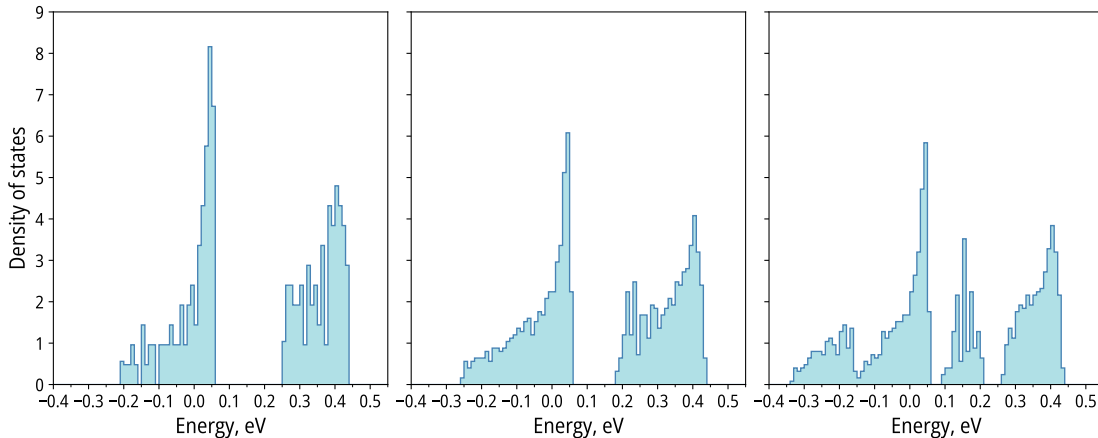


FIG. 1. Holon and doublon quasi-particle excitation eigen-energy spectra obtained using the hierarchy of correlations for the hexagonal lattice with charge disorder at $r = 26\%$ for (a) $V = 0.00$ eV (b) $V = -0.10$ eV (c) $V = -0.20$ eV.

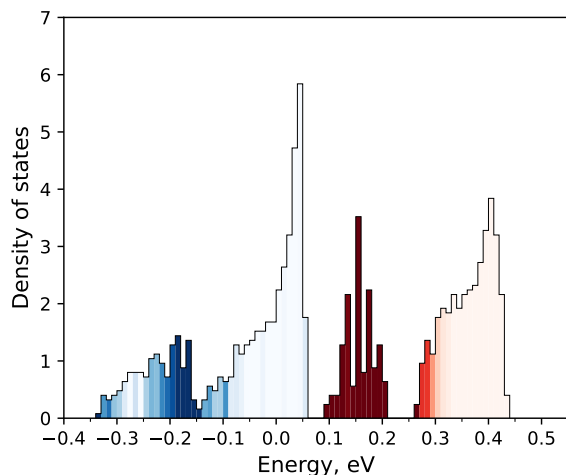


FIG. 2. Holon (blue) and doublon (red) eigen-energy spectra for charge disordered hexagonal lattice with $V = -0.20$ eV and $r = 26\%$. The shading visualises the proportion of localised states, with darker colours corresponding to more localised states.

Selected holon states are visualised in Figure 3 for different eigen-energies in the holon band. We can go a step further and plot the scaling of the participation ratio distribution as the lattice size changes - this is shown in Figure 4. Interestingly, we observe two distinct peaks in the distribution, one corresponding to very localised states, the second corresponding to delocalised states. Thus, the charge disorder directly results in the emergence of two different length scales in the system, corresponding to the typical sizes of localised and delocalised states.

Finally, note that the fine structure (peaks) in the localised doublon sub-band in Figure 2 persists also after averaging the spectrum over many disorder realisations. Physically, the central peak can be considered to be due

to single, isolated doped sites, while the surrounding two peaks arise as the symmetric and anti-symmetric states on small clusters of doped sites.

1. Square and honeycomb lattices

Comparison between hexagonal, square and honeycomb lattices offers insight into how reducing the coordination number Z affects the quasi-particle states. From a site percolation theory perspective, with the same fraction of doped sites, having fewer neighbours increases the threshold below which finite clusters dominate the physics of the system [21]. Thus, for instance, there is a noticeable difference in fraction of very localised sites between the hexagonal lattice in Figure 2 and the square and honeycomb lattices in Figures 5(a) and 5(b), respectively. This becomes even more apparent if we consider the distribution of participation ratios, Figure 6. Note that the bimodal structure observed in the previous subsection exists for all three lattice types, although the separation of the two length scales appears to be strongly dependent on the lattice type.

C. Spin-fixed background

Consider now a half-filled background where each site contains one electron with a fixed spin direction. Mathematically, this means

$$\hat{\rho}_\mu^0 \in \{|\uparrow\rangle_\mu \langle\uparrow|, |\downarrow\rangle_\mu \langle\downarrow|\}, \quad (12)$$

and correspondingly $\langle \hat{N}_{\mu, \bar{s}}^I \rangle^0 \in \{0, 1\}$ depending on the orientation of the spin at site μ . We maintain a spin-unpolarised sample, meaning $\hat{\rho}_\mu^0$ has equal probability to be either of the two options above.

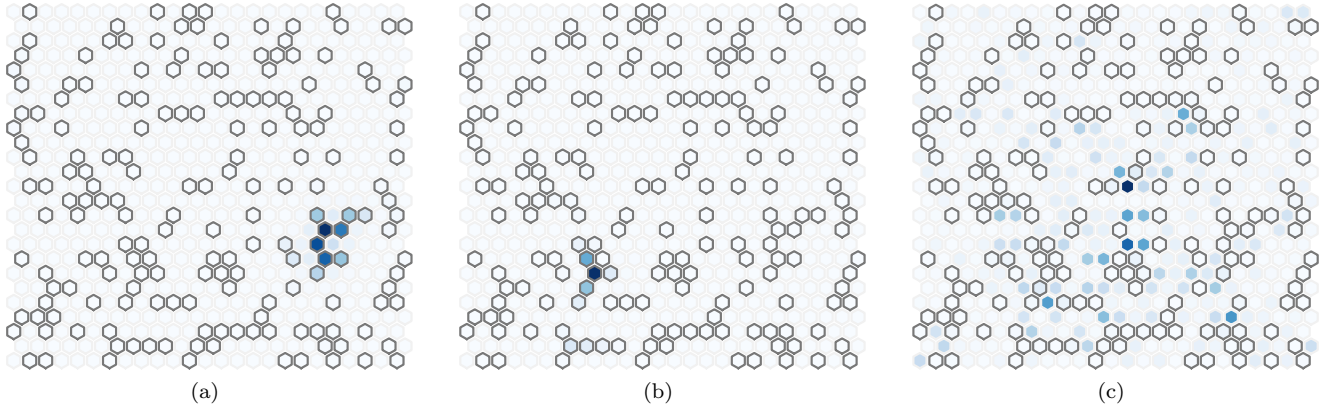


FIG. 3. Illustrations of selected holon eigen-states in the charge disordered hexagonal lattice. Dark outline corresponds to sites with on-site energy $V_\mu = V = -0.20$ eV, light outline corresponds to $V_\mu = 0$. The states have eigen-energies (a) $E \approx -0.315$ eV (bottom of doped holon sub-band) (b) $E \approx -0.161$ eV (top of doped holon sub-band) (c) $E \approx -0.031$ eV (middle of undoped holon sub-band).

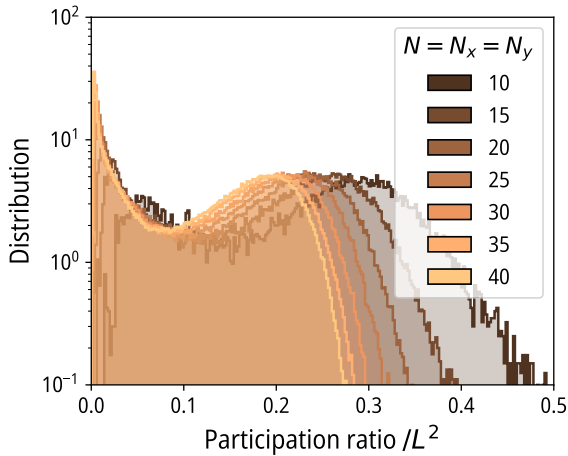


FIG. 4. Normalised distributions of the participation ratio for different lattice sizes in the case of charge disorder characterised by $V = -0.20$ eV and $r = 26\%$.

Consider now the factorised equation of motion (8). If $\langle \hat{N}_{\mu,\bar{s}}^I \rangle^0 = 0$, then we simply get diagonal evolution of $p_{\mu,s}^I$ without any coupling to adjacent sites. For example, consider a site μ which has an electron of spin s in the background. Then, $\langle \hat{N}_{\mu,\bar{s}}^1 \rangle^0 = \langle \hat{N}_{\mu,s}^0 \rangle^0 = 0$ and $\langle \hat{N}_{\mu,\bar{s}}^0 \rangle^0 = \langle \hat{N}_{\mu,s}^1 \rangle^0 = 1$. Thus, here the diagonal terms are $p_{\mu,s}^1$ and $p_{\mu,\bar{s}}^0$. We now argue that such terms should, in fact, be discarded from our consideration.

First, recall that $p_{\mu,s}^I$ is defined through the factorisation in equation (7). Considering now arbitrary $\hat{C}_{\nu,s}^{J\dagger}$ at $t = 0$,

$$s : \langle \hat{N}_{\mu,s}^1 \rangle^0 = 1 \implies (p_{\nu,s}^J)^* p_{\mu,s}^1 = \langle \hat{C}_{\nu,s}^{J\dagger} \hat{C}_{\mu,s}^1 \rangle = 0, \quad (13)$$

and hence $p_{\mu,s}^1(t = 0) = 0$. A similar consideration also fixes $p_{\mu,\bar{s}}^0(t = 0) = 0$. Then, because $p_{\mu,s}^1$ and $p_{\mu,\bar{s}}^0$ evolve

diagonally, they also stay zero at all times to this order of approximation. Physically, this is the statement that the evolution of the background is not taken into account when considering the two-point correlators to leading order in $1/Z$. Note that these effects can become important at higher orders of the hierarchy of correlations [22].

Thus, only one in each pair $\{p_{\mu,s}^I, p_{\mu,\bar{s}}^I\}$ is relevant, and in what follows we can discard the other from our considerations. Correspondingly, for the remainder of this section we omit the spin index, since this is implicitly fixed by the positional index μ and superscript I .

Finally, the relevant factorised equations for the spin-fixed background read

$$i\partial_t p_\mu^I = U^I p_\mu^I - \frac{1}{Z} \sum_\nu T_{\nu\mu} (p_\nu^I \delta_{\sigma_\mu, \sigma_\nu} + p_\nu^{1-I} \delta_{\sigma_\mu, \bar{\sigma}_\nu}), \quad (14)$$

where σ_μ is the spin at site μ . Note that, by throwing away the irrelevant p 's, we are immediately reassured that the time evolution of $p_{\mu,s}^I$ is unitary – something that we could not necessarily have concluded otherwise. Note also that the two relevant $p_{\mu,s}^I$ at each site are completely decoupled.

Note that even in this case the spectrum shows clearly distinct holon and doublon bands, see Figure 7. On the other hand, in contrast to the charge disorder case, there is no splitting of the bands into sub-bands, while localised states appear to be present at all energies within the bands, not just the band edges.

D. Combined disorder

Including both the spin disorder and charge disorder, we expect even stronger localisation of the eigen-states. This is indeed what we observe, and is most clearly seen by comparing the distributions of participation ratios for

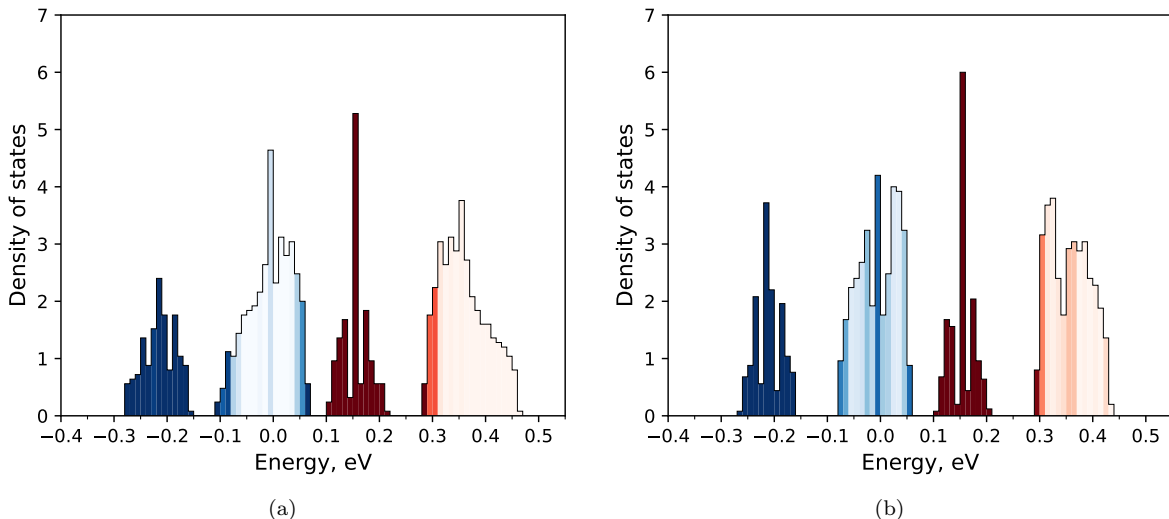


FIG. 5. Holon (blue) and doublon (red) eigen-energy spectra for charge disordered (a) square and (b) honeycomb lattices with $V = -0.20$ eV and $r = 26\%$. The shading visualises the proportion of localised states, with darker colours corresponding to more localised states.

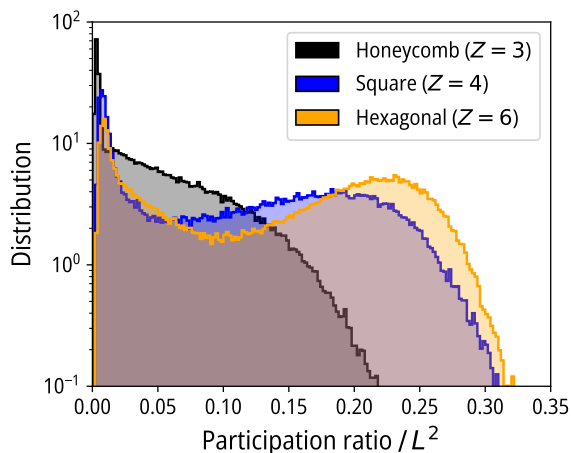


FIG. 6. Normalised distributions of the participation ratio in hexagonal, square, and honeycomb lattices with charge disorder characterised by $V = -0.20$ eV and $r = 26\%$.

the three different cases of charge disorder, spin disorder, and combined disorder, see Figure 8.

IV. PERTURBATION THEORY IN T/U

It is instructive to compare results obtained using the hierarchy of correlations with a more conventional method. To this end, we attempt to reproduce the most important points of the previous section, now from the perspective of strong-coupling perturbation theory. We focus on holon excitations on the half-filled background, and, to make the calculations tractable, restrict ourselves to first order. Further, we restrict ourselves to the single-

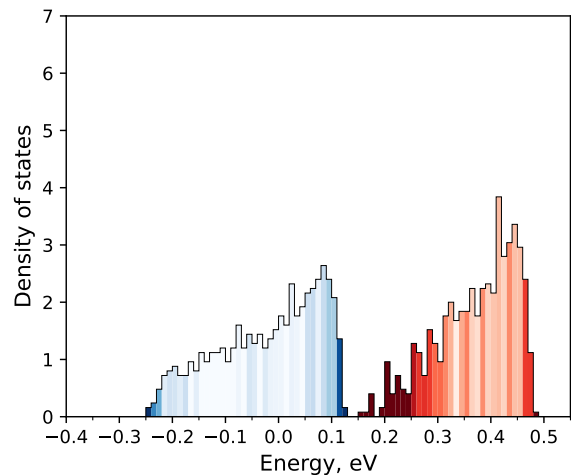


FIG. 7. Holon (blue) and doublon (red) energy spectra for spin disordered hexagonal lattice. The shading visualises the proportion of localised states, with darker colour corresponding to more localised states.

hole subspace of the full Hilbert space, meaning that we do not consider states with e.g. two holes and one doubly-occupied site. Including these would affect the energy spectrum at second order. However, this cannot be said for the eigen-states, since already for $V = -0.20$ eV we could have the energy of a state with a doubly occupied site plus two hole sites be comparable to the energy of a single hole state, $U + V \sim V$.

We work in the regime of small hopping parameter T . Consequently, our starting point in the perturbation theory are single-site states.

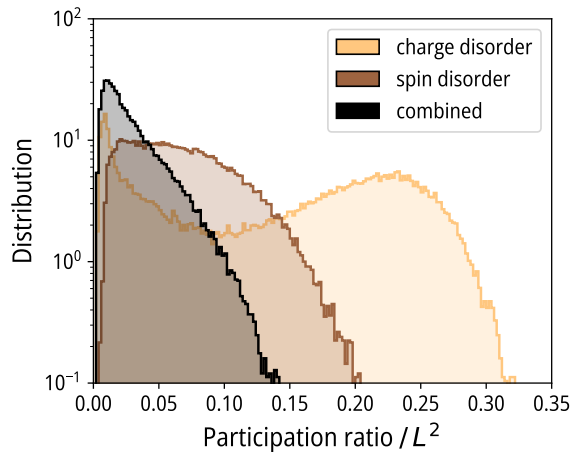


FIG. 8. Density of states versus the participation ratio for spin, charge and a combination of disorders for the hexagonal lattice. Charge disorder with parameters $V = -0.20$ eV and $r = 26\%$.

A. Charge disorder

Formally, a perturbation theory approach to a spin-disordered background would necessitate considering the entire space of states differing by permutations of the spins. However, due to the arbitrary charge disorder, this is intractable analytically and numerically for all but the smallest lattices.

As a simplified picture, we approximate the relevant dynamics by

1. imposing as a constraint on the Hilbert space that each lattice site can contain at most one fermion;
2. taking $T \rightarrow T/2$ to capture the effectively suppressed hopping in a disordered background.

As discussed, the first of these already fails when considering first order corrections to eigen-states of the system. The second is an *ad hoc* way to reproduce the correct energy spectrum in a pristine lattice. We could also motivate this by similarity with section III B.

The eigen-spectra, with sign of energy inverted to facilitate comparison with previous results, are shown in Figure 9 for $V \in \{0.00, -0.10, -0.20\}$ eV. Qualitatively, these capture the same splitting into two sub-bands observed already in Figure 1. In fact, considering also the colored spectrum for $V = -0.20$ eV in Figure 10, the structure of the localised sub-band is actually closer to that of the localised doublon sub-band obtained using the hierarchy of correlations. We expect this fine structure to be smoothed out at higher orders in perturbation theory due to mixing with states not included in our restricted Hilbert space at first order. Thus, the hierarchy of correlations at first order in $1/Z$ already captures at least

some of the effects that only appear beyond first order in perturbation theory.

B. Spin-fixed background

Consider now the half-filled background where each site contains a single fermion, its direction fixed in the ground state by the spin splitting Hamiltonian of equation (3). Figure 11 shows that perturbation theory predicts the states in the holon band to be more localised than suggested by the analogous results from the hierarchy of correlations, Figure 7. Following the discussion of the previous subsection, it can again be suggested that this is due to the hierarchy of correlations at first order in $1/Z$ capturing interactions between more states, which we have excluded from our perturbation theory analysis to make calculations in the latter tractable.

V. CONCLUSIONS AND OUTLOOK

Through an analysis based on the hierarchy of correlations, as well as a comparison with strong-coupling perturbation theory, we have analysed quasi-particle states in the half-filled Fermi-Hubbard model in the presence of charge and spin disorders. Our results show the states localising to varying degrees.

Adding spin disorder to the system restricts the types of excitations that can be present at each lattice site. The quasi-particle states localise to varying degrees, depending on how well each quasi-particle fits into the new, restricted lattice space. Consequently, localisation occurs at energies throughout the original quasi-particle bands.

An intriguing contrast to this is provided by charge disorder, which results in a distinct bimodal distribution of the participation ratios of eigen-states, indicating the emergence of two distinct length scales corresponding to localised and delocalised states. Furthermore, the localised states are observed to form localised holon and doublon sub-bands in the energy eigen-spectra. These separate energetically from what remains of the (delocalised) original quasi-particle bands, with the separation controlled by the on-site disorder potential strength V . In turn, this also indicates a spatial separation between localised states in doped regions (at potential V) and undoped regions (at zero potential).

ACKNOWLEDGMENTS

This work was funded by the Deutsche Forschungsgemeinschaft (DFG, German Research Foundation) through Project No. 278162697 (SFB 1242).

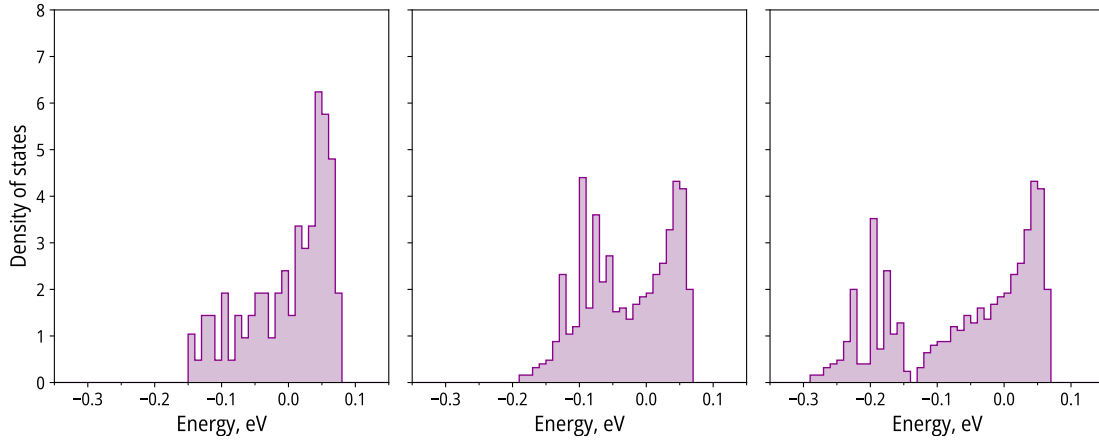


FIG. 9. Holon eigen-energy spectra obtained using perturbation theory in the hexagonal lattice with charge disorder at $r = 26\%$ for (a) $V = 0.00$ eV (b) $V = -0.10$ eV (c) $V = -0.20$ eV. To facilitate comparison with Figure 1, the density of states is divided by 2.

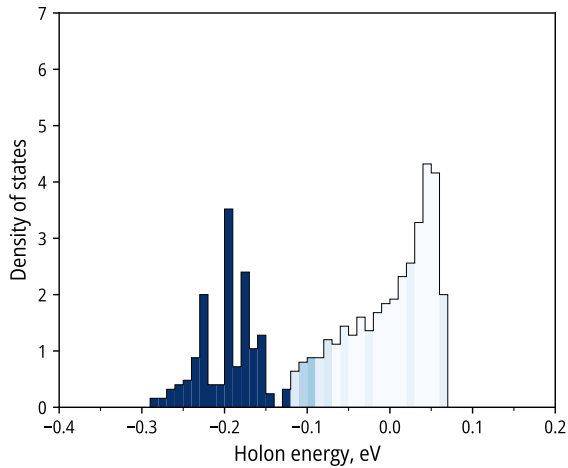


FIG. 10. Holon eigen-energy spectrum for charge disordered hexagonal lattice, coloured to reflect the localisation of states in each energy range. Darker shading corresponds to a larger proportion of localised states. To facilitate comparison with Figure 2, the density of states is divided by 2.

-
- [1] P. W. Anderson *et al.*, Absence of diffusion in certain random lattices, *Physical review* **109**, 1492 (1958).
- [2] L. Fleishman and P. W. Anderson, Interactions and the anderson transition, *Physical Review B* **21**, 2366 (1980).
- [3] A. Chabanov, M. Stoytchev, and A. Genack, Statistical signatures of photon localization, *Nature* **404**, 850 (2000).
- [4] Y. Lahini, A. Avidan, F. Pozzi, M. Sorel, R. Morandotti, D. N. Christodoulides, and Y. Silberberg, Anderson localization and nonlinearity in one-dimensional disordered photonic lattices, *Physical Review Letters* **100**, 013906 (2008).
- [5] T. Schwartz, G. Bartal, S. Fishman, and M. Segev, Transport and anderson localization in disordered two-dimensional photonic lattices, *Nature* **446**, 52 (2007).
- [6] R. L. Weaver, Anderson localization of ultrasound, *Wave motion* **12**, 129 (1990).
- [7] H. Hu, A. Strybulevych, J. Page, S. E. Skipetrov, and B. A. van Tiggelen, Localization of ultrasound in a three-dimensional elastic network, *Nature Physics* **4**, 945 (2008).
- [8] S. Kondov, W. McGehee, J. Zirbel, and B. DeMarco, Three-dimensional anderson localization of ultracold matter, *Science* **334**, 66 (2011).

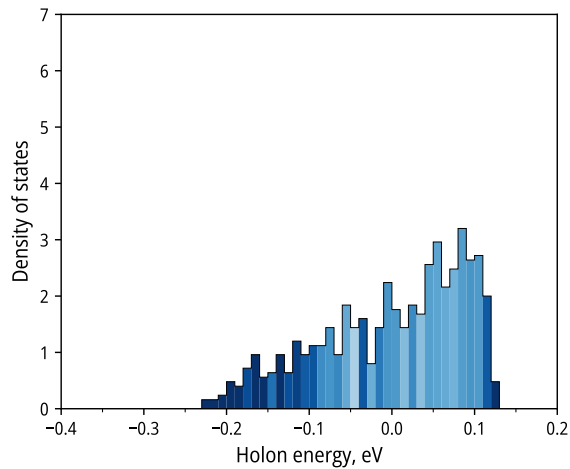


FIG. 11. Holon eigen-energy spectrum for spin disordered hexagonal lattice, coloured to reflect the localisation of states in each energy range. Darker shading corresponds to a larger proportion of localised states. To facilitate comparison with Figure 7, the density of states is divided by 2.

- [9] J. Billy, V. Josse, Z. Zuo, A. Bernard, B. Hambrecht, P. Lugan, D. Clément, L. Sanchez-Palencia, P. Bouyer, and A. Aspect, Direct observation of anderson localization of matter waves in a controlled disorder, *Nature* **453**, 891 (2008).
- [10] I. V. Gornyi, A. D. Mirlin, and D. G. Polyakov, Interacting electrons in disordered wires: Anderson localization and low-t transport, *Physical review letters* **95**, 206603 (2005).
- [11] D. M. Basko, I. L. Aleiner, and B. L. Altshuler, Metal-insulator transition in a weakly interacting many-electron system with localized single-particle states, *Annals of physics* **321**, 1126 (2006).
- [12] D. A. Abanin, E. Altman, I. Bloch, and M. Serbyn, Colloquium: Many-body localization, thermalization, and entanglement, *Reviews of Modern Physics* **91**, 021001 (2019).
- [13] S. Roy and D. E. Logan, The fock-space landscape of many-body localisation, *Journal of Physics: Condensed Matter* **37**, 073003 (2025).
- [14] M. Schreiber, S. S. Hodgman, P. Bordia, H. P. Lüschen, M. H. Fischer, R. Vosk, E. Altman, U. Schneider, and I. Bloch, Observation of many-body localization of interacting fermions in a quasirandom optical lattice, *Science* **349**, 842 (2015).
- [15] J. Hubbard, Electron correlations in narrow energy bands, *Proceedings of the Royal Society of London. Series A. Mathematical and Physical Sciences* **276**, 238 (1963).
- [16] P. Navez and R. Schützhold, Emergence of coherence in the mott-insulator-superfluid quench of the bose-hubbard model, *Physical Review A—Atomic, Molecular, and Optical Physics* **82**, 063603 (2010).
- [17] P. Navez, F. Queisser, and R. Schützhold, Quasi-particle approach for lattice hamiltonians with large coordination numbers, *Journal of Physics A: Mathematical and Theoretical* **47**, 225004 (2014).
- [18] U. R. Fischer, R. Schützhold, and M. Uhlmann, Bogoliubov theory of quantum correlations in the time-dependent bose-hubbard model, *Physical Review A—Atomic, Molecular, and Optical Physics* **77**, 043615 (2008).
- [19] R. Bell and P. Dean, Atomic vibrations in vitreous silica, *Discussions of the Faraday society* **50**, 55 (1970).
- [20] F. Wegner, Inverse participation ratio in $2 + \varepsilon$ dimensions, *Zeitschrift für Physik B Condensed Matter* **36**, 209 (1980).
- [21] J. W. Essam and M. Sykes, Exact critical percolation probabilities for site and bond problem in two dimensions, *J. Math. Phys* **5**, 1117 (1964).
- [22] F. Queisser, C. Kohlfürst, and R. Schützhold, Back-reaction and correlation effects on prethermalization in mott-hubbard systems, *Physical Review B* **109**, 195140 (2024).